Publ. Astron. Soc. Japan **42**, 279–286 (1990)

The X-Ray Spectrum of Kepler's Supernova Remnant

Isamu HATSUKADE,* Hiroshi TSUNEMI, and Koujun YAMASHITA

Department of Physics, Faculty of Science, Osaka University, 1-1, Machikaneyama-cho, Toyonaka, Osaka 560

Katsuji KOYAMA

Department of Astrophysics, Faculty of Science, Nagoya University, Furo-cho, Chikusa-ku, Nagoya 464-01

and

Yoshihiro ASAOKA and Ikuko ASAOKA

Department of Physics, Rikkyo University, Nishi-Ikebukuro, Toshima-Ku, Tokyo 171

(Received 1989 January 18; accepted 1989 November 21)

Abstract

Kepler's SNR was observed with the Large Area Counter on board the Ginga satellite in the energy range 1–12 keV. A strong iron Kα emission line has been found at 6.48±0.07 keV. This value is too low if the plasma has reached the collisional ionization equilibrium (CIE) condition and, therefore, indicates that the plasma is still in a non-equilibrium ionization (NEI) condition. Using a NEI model, we determined the electron temperature, T_e, to be 4.5±0.3 keV, and the plasma parameter, τ (the product of the electron number density n and the elapsed time t after the shock heating), to be $10^{10.24\pm0.03}$ cm^{-3} s. We also determined the abundances of heavy elements, and found that iron is overabundant by a factor of 15±2 compared to the cosmic value. The iron mass within the remnant was estimated to be about 0.01 $M_\odot$, which is less than one tenth of that predicted by the theory for Type I SN. We also discuss the differences between Kepler's and Tycho's SNRs.

Key words: Element abundance; Kepler's SNR; Supernova remnants; X-ray spectra.

* Present address: Department of Electronic Engineering, Faculty of Engineering, Miyazaki University, 1-1, Gakuen-kibanadai-nishi, Miyazaki, Miyazaki 889-21

1. Introduction

Kepler's SNR (SN 1604) is associated with one of the historical SNs; its age is nearly equal to those of Cas A and Tycho. It has been classified as a Type I SN from a study of historical records (Baade 1943). The radio maps show that Kepler's SNR is a typical shell-type SNR (Gull 1975). The radio shell is nearly circular and especially intense in the northern part. The distance is uncertain; Green (1984) discusses various distance estimation methods and concludes that a distance of 4.4 kpc is "reasonable".

An X-ray image and a spectrum were obtained with the Einstein Observatory. The X-ray image obtained with the High Resolution Imager (HRI) was qualitatively similar to that of a radio map (White and Long 1983; Matsui et al. 1984). The shell radius is 80″ and the FWHM of the shell thickness is 17″. The X-ray spectrum in the energy range of 0.8–4.5 keV obtained with the Solid State Spectrometer (SSS) shows strong emission lines from helium-like silicon, sulfur, argon and calcium (Becker et al. 1980b). These lines clearly show that the Kepler's SNR is similar to the well known shell-type SNRs, Tycho and Cas A (Becker et al. 1979, 1980a).

Hughes and Helfand (1985) reanalyzed both the spectrum and the imaging data, employing a non-equilibrium ionization (NEI) model including the hydrodynamic evolution of the SNR. They analyzed two cases: one in which most of the X-rays come from a blast wave and the other in which they come from reverse shock. They could not distinguish between these two cases from the data alone. In either case, they concluded that the mass of the progenitor must be several solar masses. They also concluded that silicon and sulfur are overabundant compared to the cosmic values by factors of 1.8 and 3.0, respectively.

Since the energy range of the SSS did not cover the iron K-line blends, the abundance of iron was deduced from the iron L-emission line blends around 1 keV. Within this energy range, the SSS could not resolve the iron L-line blends from the continuum. Therefore, observations in the energy range above 4 keV are required in order to establish the abundance of iron. We performed observations of the Kepler's SNR in the energy range 1–12 keV using the Large Area Counter (LAC) in order to clarify the emission lines above 4 keV.

2. Observation and Analysis

Kepler's SNR was observed with the LAC on board the X-ray astronomy satellite Ginga. The LAC consists of eight sets of large-area proportional counters with an effective area of 4000 cm^2 and an energy resolution of 18 % at 6 keV. Details of the Ginga satellite and the LAC have been described by Makino and the ASTRO-C team (1987) and Turner et al. (1989). All of the data were obtained in the MPC-1 mode: data are accumulated in 48 pulse-height channels in each individual counter and layer in the energy range 1–36 keV. We analyzed the data obtained from the top layers, since they are more sensitive to X-rays below 12 keV than the middle layers.

The observation of Kepler's SNR was performed on March 31, 1987 for about 7000 s. Since Kepler's SNR is near the galactic center (l=4°.8, b=6°.8), we must take into account the galactic diffuse emission for background subtraction. To investigate the galactic diffuse emission near Kepler's SNR, we performed a pointing observation

at l=6°.5,b=7°.0 on March 18, 1988 and a scanning observation along b=5°.0, l=−5°.0 to +15°.0 on March 21, 1988; we used these data (l=6°.5, b=7°.0) for background. The intensity fluctuations in the diffuse component around Kepler's SNR is less than 10 %. The count rate of the galactic diffuse component is about 6.8 counts s^{-1} (1–12 keV), while that of Kepler's SNR is about 23.6 counts s^{-1}(1–12 keV). Therefore, spatial variations in the background do not significantly affect the data analysis.

In figure 1, we show the pulse-height data obtained in this way. We can easily recognize the strong emission line around 6–7 keV. The X-ray spectrum obtained with SSS shows that the emission lines of silicon, sulfur, argon and calcium dominate below 4 keV (Becker et al. 1980b). These lines are not resolved in our data and appear as a soft excess over the continuum spectrum determined above 4 keV. We can consider that the spectrum above 4 keV is well represented by a continuum and an iron line.

First, we fit the data above 4 keV with a thermal bremsstrahlung model plus an emission line. In this model fitting, we neglected the intrinsic width of the emission line. We left the intensity and temperature of the bremsstrahlung and the intensity and the mean energy of the line as free parameters, obtaining a minimum χ^2 value of 10.0 with 7 degree of freedom (d.o.f.), which is an acceptable fit from a statistical point of view. The best-fit parameters are shown in table 1. The iron line energy is

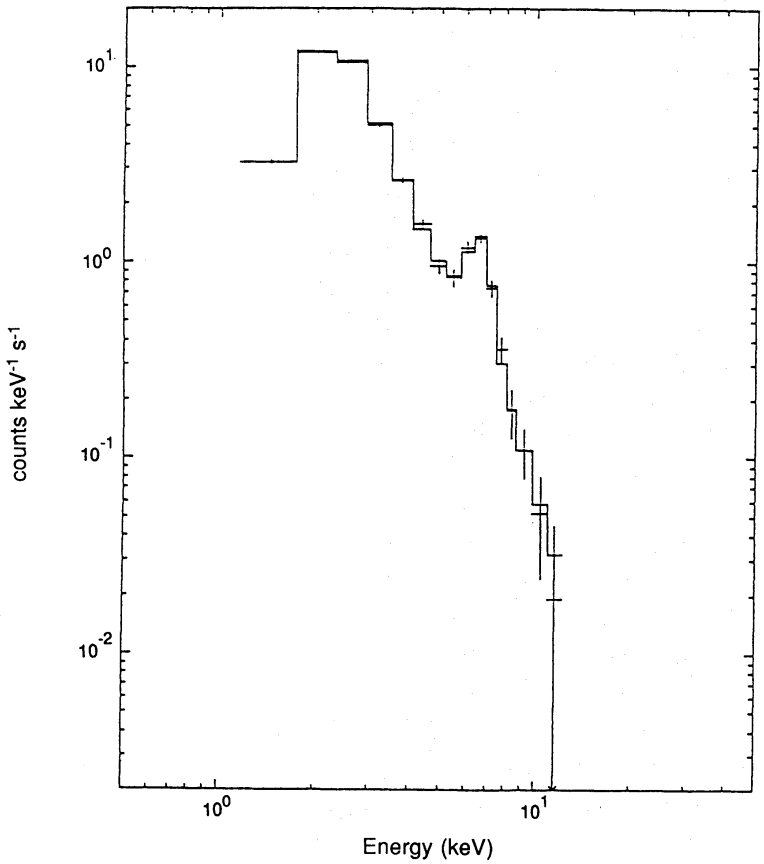

Fig. 1. X-ray spectrum for Kepler's SNR. The crosses show the pulse-height spectrum with a $\pm 1\sigma$ statistical error. The overall solid line on the data points is the best-fit NEI model folded through the detector response.

Table 1. Thermal bremsstrahlung + emission line model.

T_e (keV)	4.4 ±1.0
E_{line} (keV)	6.48±0.07
I_{line} (counts s^{-1} cm^{-2})	$0.37\pm0.05 \times 10^{-3}$
reduced χ^2	1.43
d.o.f.	7

Only the data above 4 keV were used.
Errors shown here are statistical at the 90% confidence level.

6.48±0.07 keV and the continuum temperature is 4.4±1.0 keV.

Judging from the mean energy of the emission line, it comes from the Kα line blends between helium-like iron and iron in the lower ionization stages. If the plasma is in collisional ionization equilibrium (CIE) at the observed continuum temperature, the mean energy of the iron Kα line blends should be 6.7 keV. This discrepancy indicates that the plasma is far from the CIE condition.

In general, the plasma in a young SNR cannot reach the CIE condition because the ionization time scale is longer than the SNR age (Itoh 1977; Gronenschild and Mewe 1982; Shull 1982; Hamilton et al. 1983). The degree of ionization is given by a parameter, τ, which is the product of the electron number density, n, and the elapsed time, t, after shock heating. Hamilton and Sarazin (1984b) showed that the X-ray spectra of SNRs can be well represented with spatially averaged values of τ and the electron temperature, T_e.

Second, we analyzed the data using an NEI model based on a calculation by Masai (1984). In this model we assume a hydrogen-dominant plasma. Furthermore, T_e is assumed to be constant in the plasma. Therefore, our model fitting excludes the possibility that the major part of the plasma is heavy elements, such as carbon and oxygen. We cannot distinguish these two cases from the X-ray spectrum in this energy band. We thus, employed a simple model of a hydrogen-dominant plasma. The free parameters are the emission integral (EI), τ, T_e, the interstellar absorption column density, N_H, and the abundances of silicon, sulfur, argon, calcium and iron. In this fitting, we kept the relative abundances of the first four elements equal to their cosmic values, since our data cannot resolve these emission lines, although the absolute value of the metallicity was allowed to vary. Other elements were fixed at their cosmic values (Allen 1973), since these elements do not significantly influence the present data analysis. We obtained a minimum χ^2 value of 8.5 with 10 d.o.f., which is also acceptable from the statistical point of view. The best-fit values for the parameters are summarized in table 2.

T_e derived from the second method is consistent with that obtained from the first method. The mean energy of the iron K line blends can be calculated under the assumption of the NEI model. We find that τ is $10^{10.2(+0.3,-0.8)}$ cm^{-3} s when both the mean energy of the iron Kα line blends and T_e are used. This value is consistent with that derived from the NEI model.

The average abundance of silicon, sulfur, argon, and calcium relative to cosmic val-

Table 2. NEI model.

EI (cm^{-3})	$3.9\pm 0.2\times10^{57}$
T_e (keV)	4.5 ± 0.3
τ (cm^{-3} s)	$10^{(10.24\pm0.03)}$
N_H (cm^{-2})	$10^{(21.85\pm0.04)}$
Fe*	15 ± 2
Si S Ar Ca*	8.5 ± 0.4
reduced χ^2	0.85
d.o.f.	10

Distance to Kepler's SNR was assumed to be 4.4 kpc.
Errors shown here are statistical at the 90% confidence level.
* Abundance relative to the cosmic value.

ues is 8.5±0.4, which are larger than the individual values of those elements obtained by Hughes and Helfand (1985). The intensities of the Si, S and Ar Kα lines expected from the best-fit parameters are 0.011, 0.0029, and 0.00064 photons cm^{-2} s^{-1}, which are also larger than the results of 0.0035, 0.0012, and 0.00013 photons cm^{-2} s^{-1}, respectively, obtained from the SSS observation (Becker et al. 1980b). The discrepancy between our results and those obtained with SSS suggests a lower continuum temperature component which cannot be resolved in our data. The LAC has no capability to resolve individual emission lines below 4 keV; thus, we could not distinguish these lines from the continuum. An observation with good energy resolution in the 1–10 keV region is needed to make this point clear.

3. Discussion

In young SNRs the ejecta heated by reverse shock contribute to X-ray emission (McKee 1974). The X-ray image of another well-known young SNR, Tycho, shows a double-shell structure associated with primary and reverse shock (Seward et al. 1983), while the X-ray image of Kepler's SNR shows a single-shell structure and an X-ray shell coinciding with the radio shell. This shows that the shell is mainly associated either with interstellar matter (ISM) heated by the primary shock or with ejecta heated by reverse shock. Hughes and Helfand (1985) excluded the intermediate case from their analysis based on an NEI model which included dynamics. We found that the iron in the X-ray emitting plasma is overabundant with respect to the cosmic value by a factor of 15±2. Therefore, we conclude that the X-ray emission mainly arises from the ejecta heated by reverse shock, since the overabundance of the iron in the ejecta can be attributed to nucleosynthesis in Type I supernova.

For a quantitative comparison, we derive the mass of the X-ray emitting plasma. According to a simple reverse-shock model [for example, Hamilton and Sarazin (1984a)] we can estimate the average elapsed time, $<t>$, weighted by the processed mass after the shock heating $<t>\approx(1/2)t_a$, where t_a is the SNR age . We can then estimate the average electron number density, $<n>$, from τ to be 2.9 cm^{-3}. The root-mean-square electron number density, $<n^2>^{1/2}$, is derived from the emission integral (EI),

Table 3. Plasma parameters.

SNR	Tycho*	Kepler
age t_a (years)	410	380
distance (kpc)	2.5	4.4
radius (pc)	2.9	1.7
τ ($cm^{-3}s$)	6.0×10^{9}	1.7×10^{10}
$<n>$ (cm^{-3})	0.9	2.9
$<n^2>^{1/2}$ (cm^{-3})	5.1	5.5
mass ($M_\odot$)	0.6	0.46
T_e (keV)	2.9	4.5
Fe abundance (ratio to cosmic value)	6.0	15

* Tsunemi et al. (1986).

expressed by $EI=(4\pi/3)(D\theta)^3 f <n^2>$, where D is the distance to the SNR, θ is the angular radius, and f is the geometrical plasma filling factor. Employing the plasma parameters shown in table 3 and a value for f of 0.25 for the strong shock case, we obtain an $<n^2>^{1/2}$ of 5.5 cm^{-3}. The ratio of $<n^2>^{1/2}$ and $<n>$ represents the plasma clumpiness, and is equal to 1.9. Using $<n>$, we obtained the mass of the X-ray emitting plasma to be 0.46 $M_\odot$ and that of the iron to be 1.0×10^{-2} $M_\odot$. Various plasma parameters derived in this way are summarized in table 3.

Several groups (Nomoto et al. 1984; Thielemann et al. 1986) have calculated the nucleosynthesis expected from the Type I SN model. Each model requires a large amount of iron (0.5–0.6 $M_\odot$) in order to explain its light curve. In the standard model for Type I SN, elements synthesized in the pre-SN stage are stratified in such a way that heavier elements are formed in the inner layer. This "onion skin" structure is approximately maintained in the ejecta. Therefore, the X-ray emitting plasma heated in the reverse shock does not show the average abundance of the whole ejecta. The obtained mass of iron derived from the X-ray spectrum is about one hundredth of the expected value. This discrepancy can be understood in that the reverse shock has not yet reached the iron-rich layer.

A large amount of unshocked iron is observed in SN 1006, which is also considered to be a Type I SNR. The X-ray spectrum of SN 1006 is thermal in origin, since Vartanian et al. (1985) detected emission lines of oxygen at 0.59 keV, although no emission lines have been reported around 6–7 keV (Koyama et al. 1987). However, Wu et al. (1983) found the absorption feature of Fe II in the UV band and Fesen et al. (1988) estimated an Fe II mass within the remnant of 0.015 $M_\odot$. By taking into account the iron in higher ionizing states, the mass of unshocked cold iron is expected to be few tenths of the solar mass (Hamilton and Fesen 1988). Consequently, the observed mass of the iron for X-ray observations does not always coincide with that predicted from the current theory for a Type I SN.

In table 3 we also show plasma parameters of Tycho's SNR obtained by Tenma (Tsunemi et al. 1986) for a comparison with our results. Tycho's SNR is also classified

as a Type I SNR with an age nearly equal to that of Kepler's SNR. According to plasma parameters τ and T_e, the iron in Tycho's SNR is in a lower ionization stage than that of Kepler's SNR. Using the plasma parameters we can calculate the iron L-emission lines distributed in the energy range of 0.7–1.3 keV. In this energy range, most of the emission is not from the continuum, but from individual lines, particularly from iron L-emission lines. The emissivity of iron for these lines of Kepler's SNR is 6.0×10^{-10} photons cm^3 s^{-1}, about 2.8 times larger than that for Tycho's SNR. Taking into account the abundances for these SNRs, we expect a large difference in the iron L-emission line features. Unfortunately our data do not cover this energy range. However, observations with the SSS (Becker et al. 1980a, b) indicate a clear difference between the two remnants. We notice that the X-ray spectrum of Kepler's SNR has a strong hump around 1 keV while that of Tycho does not, which is consistent with our result.

4. Conclusion

We have obtained the X-ray spectrum of Kepler's SNR in the energy range 1–12 keV. We found strong iron Kα emission-line blends at 6.48±0.07 keV. This value for the energy clearly shows that the plasma is in the ionizing phase. By applying a simple NEI model to the data, we obtain a plasma parameter, τ, of $10^{10.24\pm0.03}$ cm^{-3} s and the electron temperature, T_e, of 4.5±0.3 keV. We derived the abundance of iron in the X-ray emitting plasma to be 15±2 times that of the cosmic value. The total amount of iron is less than that predicted by the theory for a Type I SN, indicating that reverse shock has not yet reached the iron-rich layer.

We acknowledge all of the members of the Ginga team for spacecraft operation and data reduction. We thank Dr. J. Hughes for his useful comments on the manuscript.

References

Allen, C. W. 1973, *Astrophysical Quantities*, 3rd ed. (The Athlone Press, London).
Baade, W. 1943, *Astrophys. J.*, **97**, 119.
Becker, R. H., Boldt, E. A., Holt, S. S., Serlemitsos, P. J., and White, N, E. 1980b, *Astrophys. J. Letters*, **237**, L77.
Becker, R. H., Holt, S. S., Smith, B. W., White, N. E., Boldt, E. A., Mushotzky, R. F., and Serlemitsos, P. J. 1979, *Astrophys. J. Letters*, **234**, L73.
Becker, R. H., Holt, S. S., Smith, B. W., White, N. E., Boldt, E. A., Mushotzky, R. F., and Serlemitsos, P. J. 1980a, *Astrophys. J. Letters*, **235**, L5.
Fesen, R. A., Wu, C. C., Leventhal, M., and Hamilton, A. J. S. 1988, *Astrophys. J.*, **327**, 164.
Green, D. A. 1984, *Monthly Notices Roy. Astron. Soc.*, **209**, 449.
Gronenschild, E. H. B. M., and Mewe, R. 1982, *Astron. Astrophys. Suppl.*, **48**, 305.
Gull, S. F. 1975, *Monthly Notices Roy. Astron. Soc.*, **171**, 237.
Hamilton, A. J. S., and Fesen, R. A. 1988, *Astrophys. J.*, **327**, 178.
Hamilton, A. J. S., and Sarazin, C. L. 1984a, *Astrophys. J.*, **281**, 682.
Hamilton, A. J. S., and Sarazin, C. L. 1984b, *Astrophys. J.*, **284**, 601.
Hamilton, A. J. S., Sarazin, C. L., and Chevalier, R. A. 1983, *Astrophys. J. Suppl.*, **51**, 115.

Hughes, J. P., and Helfand, D. J. 1985, *Astrophys. J.*, **291**, 544.
Itoh, H. 1977, *Publ. Astron. Soc. Japan*, **29**, 813.
Koyama, K., Tsunemi, H., Becker, R. H., and Hughes, J. P. 1987, *Publ. Astron. Soc. Japan*, **39**, 437.
Makino, F., and the ASTRO-C team 1987, *Astrophys. Letters. Commun.*, **25**, 223.
Masai, K. 1984, *Astrophys. Space Sci.*, **98**, 367.
Matsui, Y., Long, K. S., Dickel, J. R., and Greisen, E. W. 1984 *Astrophys. J.*, **287**, 295.
McKee, C. F. 1974, *Astrophys. J.*, **188**, 335.
Nomoto, K., Thielemann, F.-K., and Yokoi, K. 1984, *Astrophys. J.*, **286**, 644.
Seward, F., Gorenstein, P., and Tucker, W. 1983, *Astrophys. J.*, **266**, 287.
Shull, J. M. 1982, *Astrophys. J.*, **262**, 308.
Thielemann, F.-K., Nomoto, K., and Yokoi, K. 1986, *Astron. Astrophys.*, **158**, 17.
Tsunemi, H., Yamashita, K., Masai, K., Hayakawa, S., and Koyama, K. 1986, *Astrophys. J.*, **306**, 248.
Turner, M. J. L., Thomas, H. D., Patchett, B. E., Reading, D. H., Makishima, K., Ohashi, T., Dotani, T., Hayashida, K., Inoue, H., Kondo, H., Koyama, K., Mitsuda, K., Ogawara, Y., Takano, S., Awaki, H., Tawara, Y., and Nakamura, N. 1989, *Publ. Astron. Soc. Japan.*, **41**, 345.
Vartanian, M. H., Lum, K. S. K., and Ku, W. H. M. 1985, *Astrophys. J. Letters*, **288**, L5.
White, R. L., and Long, K. S. 1983, *Astrophys. J.*, **264**, 196.
Wu, C.-C., Leventhal, M., Sarazin, C. L., and Gull, T. R. 1983, *Astrophys. J. Letters*, **269**, L5.